POLITECNICO
MILANO 1863

SCUOLA DI INGEGNERIA INDUSTRIALE
E DELL'INFORMAZIONE

EXECUTIVE SUMMARY OF THE THESIS

Synthesis and characterization of colloidal antimony sulfobromide (SbSBr) nanocrystals.

LAUREA MAGISTRALE IN MATERIALS ENGINEERING AND NANOTECHNOLOGY – INGEGNERIA NANOMATERIALS AND NANOTECHNOLOGY.

AUTHOR: SRAVAN ERKULLA

ADVISOR: METRANGOLO PIERANGELO

CO-ADVISOR: CARLO GIANSANTE

ACADEMIC YEAR: 2022-2023

1. Aim of the Thesis.

This thesis work aims to address some of the major issues faced during the synthesis of colloidal nanocrystals (NCs). Primarily, by considering Antimony Sb^{+3}, as a non-toxic[1], high absorption coefficient and efficient charge carrier mobility element[2–4]. Besides, the selection of a suitable method for the synthesis of pure phase and stable NCs, was addressed by opting colloidal growth method, through which we have try to understand the following, transformative mechanism from the precursor/reagents stage to the well-confined NCs which include, phase transformation and surface passivation of NCs. Lastly, by carrying out a suitable investigating procedure, by conducting some optical, morphological, and structural characterization works to validate the obtained Antimony sulfobromide NCs, is to identify its credibility for further embedment in devices.

2. Introduction

As synthesis of colloidal NCs is extremely an active area of research in materials science for the development of unprecedented functional materials. The major consequences which were faced during the synthesis of colloidal NCs are the control over chemical composition, size and shape and their stability.

In the recent times the demand for the energy and its production is being increasing day to day. In order to meet the current demand, the optimal and

efficient PV material need to be utilized which can sustain the environmental conditions naturally. In this end, ternary metal chalcogenide PV material was introduced, which exhibit better physico-chemical properties and be stable in harsh environments, as wide band gap, effective absorption coefficient, and optical properties can be tailored. When compared with the ternary metal halide PV material, with high electro-negative element, possess narrow band gap and highly efficient materials with structural instabilities, which makes these materials to not to last longer.

As the metal chalcogenide possesses better qualities in order to be still maintained in energy harvesting industry, a split anion exchange method was taken into consideration for the introduction of the metal chalcohalide PV material. In order to address these, a ternary metal chalcohalide need to be replaced with the above PV materials. The ternary (heavy pnictogen) metal chalcohalide are considered on the following basis, high-Z ns^2 electron configuration and during the interaction with electromagnetic radiation, the occurrence of spin-orbit coupling which enhances the polarization of the charge carriers in semiconductors with some basis of (ferroelectrics) Pb^{+2} cation for consideration, and with similar conditions, even upon the ability in forming +3 charge, despite this, heavy pnictogen elements ($Sb^{3+,}$ and Bi^{3+}) makes a suitable consideration for charge generation and transfer conditions. Moreover, they offer poor dichotomy, structural stability in harsh environments, and high charge carrier mobility, which pushes these materials as a promising alternative with non-toxic and earth-abundant characteristics, when compared to the Lead halide-based and hybrid-perovskites for photovoltaics[2,5].

Moreover, due to the distinctive electronic structure in chalcohalides, which arises the anti-bonding condition, upon hybridization of s-p orbitals, obtained by valence band maximum of the cation with the conduction band minimum of anion, which exhibits defect tolerant and high charge carrier mobility situation. The involvement of multiple anions i.e., mono-valent and di-valent elements, allow for the tailoring of the chemical composition of chalcohalide-based compounds, which leads to the usage of these nanocrystals in multiple applications. Synthesis of inorganic nanocrystals through synthetic procedures limits their usage in device fabrication due to their poor post-synthesis processibility, from the above synthesis issues, stability, and suitable characteristics in order to be accompanied in PV industry were addressed.

3. Methods.

3.1. Synthesis Method.

In general synthesis of NCs is a major inter play between the physics and chemistry. Over the last two decades, nanocrystals are synthesized through various methods which are mainly categorized under; 1. Top-down and 2. Bottom-up approach.

In the top-down method, the nanocrystals are attained through the reduction of micro (bulk) particles to the nanoscale level, by using various methods such as milling, etching etc. From the above procedure, the individual cannot attain the required composition and the size/shape of the nanocrystals easily or alter according to the desired composition needed. To control the above, bottom-up approach is followed on which the desired composition and structure is obtained from their constituent atoms, which ends up producing colloidal nanocrystals, in the current thesis work we have followed the bottom-up approach in order to attain the tailored materials[6].

3.1.1. Hot-injection synthesis of semiconductor NCs.

Hot-injection synthesis technique is majorly used in respect to the attainment of the highly monodisperse (nearly >95%) NCs and tailored procedures to receive defect free nanocrystals.

In the present technique as said above, reagents, stabilizing agents and solvent are added in a three neck round bottom flask and heated-up the added flask to the desired temperature (i.e., reaction temperature (RT) 150°C-230°C) with the help of a heating mantle. The reaction procedures were done in a controlled and in an ambient condition such as, considerable vacuum and continuous nitrogen purging is maintained in a well-defined Schlenk line setup, which is done to avoid the oxidation and hydrolysis in the reaction flask, moreover constant observation of the temperature in the reaction flask is followed.

As the core surfactant precursors are added into the reaction flask, supersaturation of monomers occur which is leading to instant or rapid nucleation also known as burst nucleation, followed by phase growth, which were in-detail explained in the LaMer and Ostwald mechanism of growth(ref.).

3.2. Characterization Method.

In a condition to validate the synthesized NCs and to figure out the characteristic properties, we have gone for morphological, structural, and optical characterization techniques.

The structural characterization was carried out by using XRD-equipment. Powder XRD patterns were received, using Panalytical Empyrean diffractometer operated in a parallel beam position way and embedded with a 1.8 kW Cu Kα ceramic X-ray (45 kW), 1 mm wide incident and receiving slits, a 40 mA PIXcel3D 2 x 2 area detector. Samples were prepared for the analysis by precipitating the crude NCs and redispersing them in toluene, the resulting product solution is drop casted on the zero-diffraction silicon substrate and dried at room temperature.

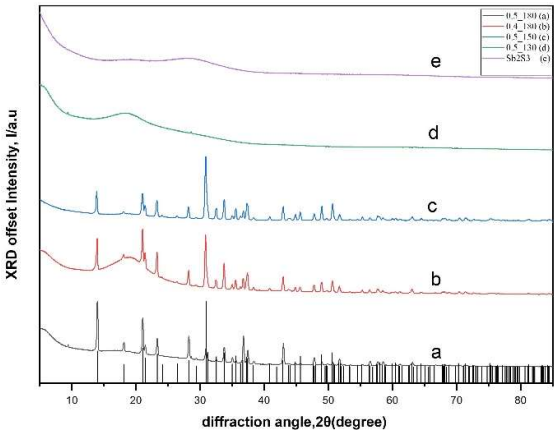

Fig. 1 Offset intensity patterns of XPD data of 0.5_SbSBr at 180°C, 0.4_SbSBr at 180°C, 0.5_SbSBr at 150°C, 0.5_SbSBr at 130°C, and Sb_2S_3 NCs at 180°C[7,8].

Morphological characterization was executed with the help of TEM equipment for which, the samples were prepared by dispersing dilute solutions of NCs (maintained in a N2-protected glovebox) onto carbon-coated grids and proceeded with the evaporation of solvent at room temperature. Low-resolution TEM images were acquired with JEOL microscope, JEM – 1400Plus, operating at 120 kV, respectively.

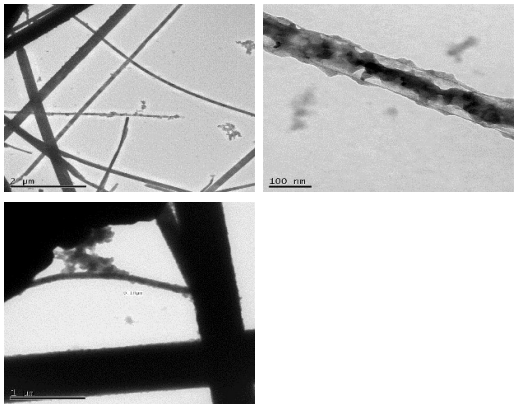

Fig. 2. TEM image of 0.5_SbSBr at 180°C, 0.4_SbSBr at 180°C, and 0.5_SbSBr at 150°C.

3.3. Optical characterization.

Due to the absorption spectroscopy, it is possible to study the optical properties of nanocrystalline semiconductors. As in the quantum confinement regime, the system generates discrete energy levels in analogy with the problem of the particle in a box/sphere. The optical absorption characteristics of a semiconductor QDs are governed by the energy-level structure of the bound excitons. In the absorption experiment the optically undergoing transitions from the ground state to the various electron–hole pair states are probed.

The samples prepared for the UV-Vis spectroscopy is by, dispersing the cleaned NCs in toluene into a measuring cuvette. At a range of wavelength from 280 to 800 nm.

4. Synthesis of Antimony sulfobromide (SbSBr) NCs.

4.1. Materials.

The materials mentioned are with high purity or with the specific concentration mentioned below and they are used as received. Antimony (III) acetate ($Sb(Ac)_3$ 99.99%, Sigma Aldrich), 1-octadecene ($C_{18}H_{36}$ 90%, Alfa Aesar), Oleic acid (OA) (RCOOH 90%, Sigma Aldrich), bis(trimethylsilyl)sulfide ($(CH_3)_3Si)_2S$ ≥98%, Sigma Aldrich), Benzyl bromide (BzBr 97%, Acros organics), 1-dodecanethiol (DoSH ≥97%, Sigma Aldrich), Dodecyldimethylammonium bromide ($Me_2Do_2N^+S^-$ ≥98% Sigma Aldrich).

The other anhydrous solvents which were used are acetone, toluene, and methanol (technical grade).

4.2. Synthesis of SbSBr NCs.

In order to attain the pure phase SbSBr NCs we have optimized the synthesis aspects such as, temperature (temp.), reaction time, and concentration (conc.).

During the initial experiment we have used the equal equivalents of the reagents such as, 0.15mmol $Sb(Ac)_3$, 0.15mmol of OA, 0.15mmol $(CH_3)_3Si)_2S$, and 0.15mmol of BzBr, with the current composition, we have ended up in obtaining **Stibnite (Sb_2S_3)**[9] NCs.

In order to overcome the above phase, we have changed the conc. of the precursors. During which, we could obtain the pure phase i.e., orthorhombic structure, Pnam/62 space group, with the following composition 0.5 mmol $Sb(Ac)_3$ and 0.4 mmol $Sb(Ac)_3$. The ratio between the both anions to the metal are maintained, Sb_2S_3: $SbBr_3$ from 1:1 to 1:10 were executed for the end limits evaluation of the composition, which could be utilized for the synthesis of SbSBr NCs.

By following the above synthesis procedures and by maintaining the Sb_2S_3: $SbBr_3$ ratio 1:6 to 1:8 we attained SbSBr NCs, but the effective composition was 1:7 ratio of Sb_2S_3 to $SbBr_3$.

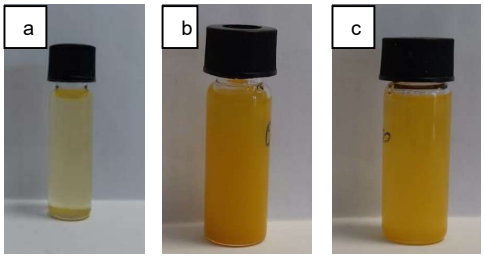

Fig. 3. a, b, and c are the images of as-synthesized SbSBr NCs with 0.5mmol, 0.4 mmol and at 150°C.

4.3. Results.

4.3.1. Morphological analysis

By using TEM equipment, we have analyzed the morphology of the NCs. Through this analysis we have identified about the sufficient amount of precursors requirement for the reaction chain to be carried out. As it was explained in the LaMer and Oswald theories, the availability of the precursor agents near the growing NC is mandatory to attain a suitable structure and size.

The NCs obtained with 0.4 mmol of $Sb(Ac)_3$ are of with the following dimensions length ≈6µm and width ≈100nm. These NCs were included with a certain polydispersity, it was at a ratio which cannot be exempted with regular cleaning technique. In order to attain the pure phase, we have increased the conc. of the metal content in the reaction chamber i.e., 0.5mmol $Sb(Ac)_3$, which yielded better than the 0.4mmol $Sb(Ac)_3$ and with the following dimensions, length ≈6µm and width ≤100nm. And the obtained monodispersed NCs are with an index of ≈95%. To evaluate the temp. aspect optimized synthesis of SbSBr NCs, we have reduced the reaction temp. i.e., to 150°C. In which the yield obtained is higher, when compared to the other two reaction compositions, after morphological analysis, it was revealed that the major portion yielded was an amorphous SbSBr NCs. The dimensions attained through this reaction were as follows, length ≈6µm and width ≥100nm.

4.3.2. Structural analysis.

The obtained XPD pattern was refined using the GSAS-II software, upon attribution of the obtained pattern with the existing data using QualX 2.0, with a match received with the JCPDS card n^0. 00-231-0798, which states that the obtained NCs are with orthorhombic structure with Pnma/62 space group and made us clear that no other phase availability in the obtained sample.

During the observation of the XPD pattern of 0.5_SbSBr at 180°C, 0.4_SbSBr at 180°C, and 0.5_SbSBr at 150°C had an observation of the 2θ angle and intensity shift (which is under negligible value). The shift in the lattice coordinates of the obtained sample with the standard crystal structure were also reported below.

Lattice parameter	JCPDS n^0. 00-231-0798	Obtained XPD data	Variation %
a	8.2600	8.3023	0.51
b	9.7900	9.7790	0.112
c	3.9700	3.9400	0.754

Table 1. Observation of the variation obtained in the synthesized 0.5_SbSBr at 180°C lattice parameters[7,8].

4.3.3. Optical analysis.

Colloidal SbSBr NCs have shown an efficient optical property i.e., absorption condition in the range of encouragement, when in comparison to other lead-based chalcogenide and halide PV materials it is an acceptable one, for approach. In order to execute the optical properties on our metamaterial, we have dispersed the sample in toluene, in order to undergo the absorption and scattering upon the incident of light. The obtained absorption spectra were used to estimate the NC indirect band gap, which is 1.80eV (0.5-SbSBr at 180°C). The direct band gap is expected to be near close to the indirect band gap, which was 2.18eV (0.5-SbSBr at 180°C).

It was observed that as we increase the halide Conc., the energy gap between the two levels

decreases, and the range of absorption conditions also varies accordingly.

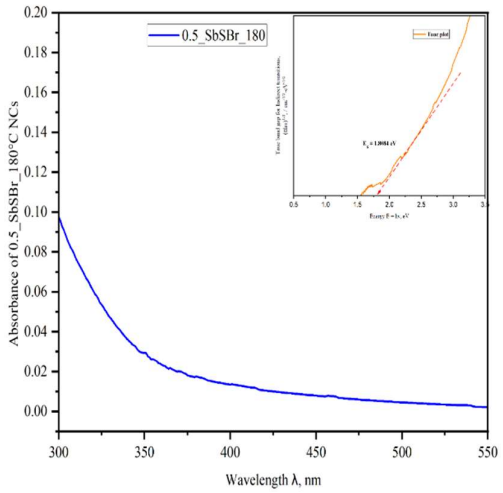

Fig. 4. Absorbance of 0.5-SbSBr at 180°C with band gap using the Tauc plot.

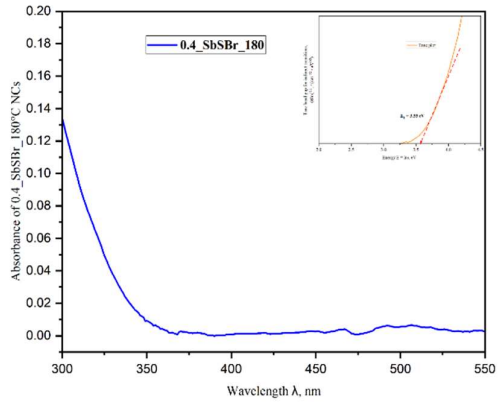

Fig. 5. Absorbance of 0.4-SbSBr at 180°C with band gap using the Tauc plot.

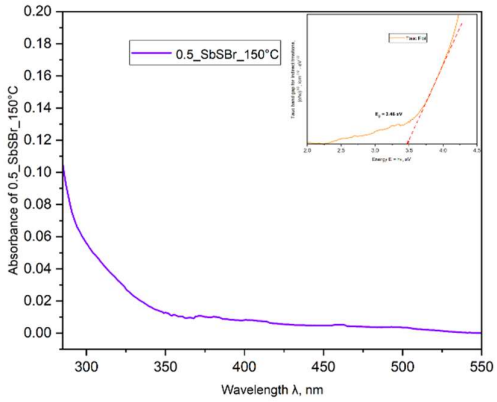

Fig. 6. Absorbance of 0.4-SbSBr at 180°C with band gap using the Tauc plot.

4.3.4. Theoretical calculations.

To validate the band gap, which was estimated using the UV-Vis spectroscopy data, and by following Lambert-beer law, we have received a value of 1.8084 eV.

So, I have used Quantum espresso- Burai (GUI) for the calculation of the band structure and the energy levels of the 0.5_SbSBr NCs at 180°C. During which I have maintained the following conditions for the execution of the algorithm to carry out on 0.5_SbSBr at 180°C, the cutoff wave frequency kept is 408.2 eV and cutoff charge is 4081.71 eV. As the shape of attained NCs are rod like structured, I have used excessive k-points in the c-axis. I have neglected the SOC condition while the execution.

The majority of the charge transfer/generation bands were from Sb and S. Through the above calculations the obtained difference in the band gap is nearly 300meV. The band gap obtained is 1.7662 eV (UV-Vis = 1.8084eV).

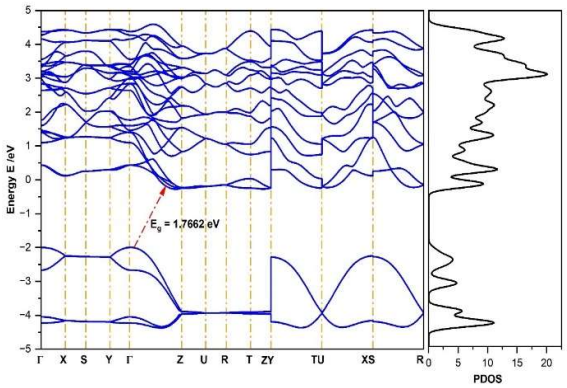

Fig. 7. Computed band gap structure and density of states of SbSBr, along with the PDOS.

4.3.5. Stability and Surface Chemistry.

The stability and the surface chemistry of the obtained NCs were analyzed using the FTIR spectroscopy. In which we have identified that the availability of the following peaks which define the availability of Sb-Oleates on the surface of the NCs.

At 3000 cm^{-1} we have observed a C-H stretching peak, at 1700 cm^{-1} and at 1400 cm^{-1}, we have observed other peaks related to the stretching energy levels of C=O. As the prominence of the availability of the above defined stretching peaks in the FTIR analysis, had clarified about the availability of the surface ligands over the grown NCs.

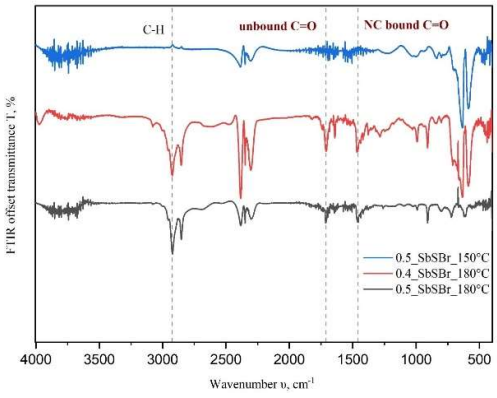

Fig. 8. FTIR spectra of 0.5-SbSBr NCs at 180°C, capped with oleic acid[3,10].

5. Conclusion.

In our synthetic approach, we have developed a stable SbSBr NCs, within the range of nano scale. The approach towards these non-toxic NCs were validated by performing, morphological, structural and photo-physics analysis and to the end surface chemistry of the SbSBr NCs was done. And the results which we have obtained were in an acceptable range of various applications such as, photovoltaics, photocatalysts and photo-electrochemistry. Moreover, the large optical band absorption coefficients in the range of visible spectrum range, made these metamaterials as prominent solar absorbers. In addition to the above, the stable condition of the NCs in ambient condition, revealed about their integration into various device electronics.

To the further extent, the current nanocrystals (NCs) can be confined to a particular range of dimensional magnitude, by introducing the growth terminating and size-shape controlling agents in the reaction mixture, which is an un-explored part in the current thesis work, which requires further investigations to carry out.

Further validation and investigation of SbSBr NCs were not performed due to time constrain, which will be addressed soon on another platform.

6. References.

1. Sun, Y.-Y. *et al.* Discovering lead-free perovskite solar materials with a split-anion approach. *Nanoscale* **8**, 6284–6289 (2016).
2. Ghorpade, U. V. *et al.* Emerging Chalcohalide Materials for Energy Applications. *Chem Rev* **123**, 327–378 (2023).
3. Quarta, D. *et al.* Colloidal Bismuth Chalcohalide Nanocrystals. *Angewandte Chemie International Edition* **61**, (2022).
4. Moreels, I. *et al.* Composition and Size-Dependent Extinction Coefficient of Colloidal PbSe Quantum Dots. *Chemistry of Materials* **19**, 6101–6106 (2007).
5. Choi, Y. C. & Nie, R. Heavy pnictogen chalcohalides for efficient, stable, and environmentally friendly solar cell applications. *Nanotechnology* **34**, 142001 (2023).
6. LaMer, V. K. & Dinegar, R. H. Theory, Production and Mechanism of Formation of Monodispersed Hydrosols. *J Am Chem Soc* **72**, 4847–4854 (1950).
7. T. Inushima and K. Uchinokura. X-ray structural analysis of ferroelectric antimony sulfobromide. *Jpn J Appl Phys* **24**, 600–602 (1985).

8. G.D. Christofferson and J.D. McCullough. The crystal structure of antimony(iii) sulfobromide, sb s br. . *Acta Crystallographica* **12**, 14–16 (1959).
9. Balakrishnan, S. K., Parambil, P. C. & Edri, E. Mechanistic Insight into the Topotactic Transformation of Trichalcogenides to Chalcohalides. *Chemistry of Materials* **34**, 3468–3478 (2022).
10. Quarta, D. *et al.* Stable Ligand Coordination at the Surface of Colloidal CsPbBr 3 Nanocrystals. *J Phys Chem Lett* **10**, 3715–3726 (2019).

7. Acknowledgement.

I would like to take this opportunity to thank my supervisor Dr. Carlo Giansante (CNR-Nanotec, Lecce) for his endless support. I also like to thank my academic supervisor Prof. Dr. Pierangelo Metrangolo for the support which he had provided for the execution of this thesis work at CNR-Nanotec. Moreover, I like to show my gratitude by thanking the people supported me in this thesis work from CNR-Nanotec and Polimi. To the end, never the less which I receive from my family, thank you.